Extraction and characterization methods for titanium dioxide nanoparticles from commercialized sunscreens

Article *in* Environmental science. Nano · November 2017

DOI: 10.1039/C7EN00677B

CITATIONS
0

READS
119

6 authors, including:

Oliver Clemens
Technische Universität Darmstadt
73 PUBLICATIONS **408** CITATIONS

SEE PROFILE

Extraction and characterization methods for titanium dioxide nanoparticles from commercialized sunscreens

Allan Philippe,[a*] *Juraj Košík*,[b] *Alexander Welle*,[c] *Jean-Michel Guigner*,[d] *Oliver Clemens*,[e] *Gabriele E. Schaumann*[a]

* Corresponding author (phone: +49-6341 280 31589, email: philippe@uni-landau.de).

[a] Group of Environmental and Soil Chemistry, Institute for Environmental Sciences, University of Koblenz-Landau, Fortstrasse 7, 76829, Landau, Germany.

[b] Faculty of Chemistry, Brno University of Technology, Antonínská 548/1,601 90, 75007 Brno, Czech Republic.

[c] Institut für Funktionelle Grenzflächen, Karlsruhe Nano Micro Facility, Karlsruhe Institute for Technology, Hermann-von-Helmholtz-Platz 1, 76344, Eggenstein-Leopoldshafen, Germany.

[d] Institut de Minéralogie, de Physique des Matériaux et de Cosmochimie (IMPMC), Sorbonne Universities - UPMC University Paris 06, UMR CNRS 7590, MNHN, IRD UR 206, 75252 Paris cedex 05, France.

[e] Faculty of Material Science, Technische Universität Darmstadt, Materials Design by Synthesis, Alarich-Weiss-Straße 2, 64287, Darmstadt, Germany.

Abstract

Sunscreens are an important source of TiO_2 nanoparticles in surface waters. The fate and toxicity of those particles have not been fully addressed due to the gap between model nanoparticles usually used in studies and the more complex particles found in commercial products. Therefore, mild extraction methods for TiO_2 nanoparticles from sunscreens were evaluated for providing more realistic nanoparticles samples for future studies. We propose two methods based on ultrafiltration and ultracentrifugation, respectively, for extracting TiO_2 nanoparticles from sunscreens using a surfactant solution as solvent. These methods were tested on eleven commercial sunscreens with differing compositions. The ultracentrifugation variant allows extracting 250 mg from approximately 5 g of sunscreen in one day. Recoveries for ultrafiltration and ultracentrifugation were 52-96% and 78-98%, respectively. Purification efficiency was determined for the ultracentrifugation variant by determining the avobenzone concentration in sunscreen extracts using UV-spectrometry and was high for all tested sunscreens. Transmission electron microscopy and dynamic light scattering revealed a high diversity in particle shape, although size parameters were comparable (average hydrodynamic diameter: 19-34 nm).

Isoelectric points were below 4.6 for all sunscreen extracts. Time-of-flight secondary ion mass spectrometry revealed that probably all TiO_2 particles were coated; most of them with PDMS, some others with Al- and Si-based materials. Comparison of images of particles inside the sunscreens using cryogenic transmission electron microscopy and of extracted particles showed that while the shape of primary nanoparticle was not affected by the extraction, they were agglomerated inside the sunscreens. These agglomerates could be completely disrupted using ultrasonication. Therefore, the particles extracted in the present study can be considered as more environmentally relevant in terms of size, shape, surface charge and coating compared to model TiO_2 nanoparticles.

Keywords

TiO_2, extraction, sunscreen, surface coating, cryogenic TEM, ToF-SIMS, isoelectric point

Introduction

The use of TiO_2 in sunscreens results in significant release of TiO_2 particles directly into surface or sea water by bathers (1). In addition, a portion of the TiO_2 particles released in waste water passes the waste water treatment plant (2). Therefore, these particles are expected to accumulate in the environment, where they could have toxic effects towards some organisms at concentrations in the ppm range (3,4). Considering recent estimations, such concentrations can be expected after accumulation of the particles in the sediments (5). However, many uncertainties are related to these estimations. One major uncertainty is the transfer of current results from fate and toxicity studies obtained for model TiO_2 particles to the case of complex nanoparticles used in commercial products. For instance, many studies addressed the fate or toxicity of photocatalytic TiO_2, especially P25, although it is not in use as such in cosmetics (6–8). While some recent studies used starting materials used by the cosmetic industry such as T-lite (7,9) or NM-103/104 (10), for instance, there is still a lack of studies addressing the fate and effects of TiO_2 nanoparticles after processing into the final product.

In order to fill this gap, studies using particles present in commercial products for studying their fate and effects in the environment are needed. Recent estimations showed that TiO_2 from sunscreen products represents 90 % of the total income of TiO_2 into freshwater (1.6 tons per year) in Denmark (11). Therefore, particles used in sunscreens are highly relevant for environmental studies. Studies of TiO_2 used in cosmetics revealed that specific aging processes (e.g. coating degradation) can be observed in environmental media (7,9). However, particle

characteristics can vary strongly from one product to another. Hence, extracting realistic TiO_2 particles directly from commercial products would be highly useful to improve the prediction quality of environmental studies.

Only few extraction methods for nanoparticles from complex matrices have been reported. Ag, Au, and Pt nanoparticles were extracted from biological tissues and soil using chemical or enzymatic digestions and/or ultrasonication (12–18). However, enzymatic or acid digestion cannot be used with sunscreens as the former would be inefficient, whereas particle coating could be damaged by acids. Furthermore, separation techniques such as field flow fractionation are efficient for size measurement and quality control (19–22), but they are not practicable for preparative purpose, and would require an instrument solely dedicated to continuous sample separation (23). More promising approaches involve organic solvents (chloroform, methanol, tetrahydrofuran and hexane) and in some cases ultrasonication or heating to disperse sunscreen prior to the purification of the particulate fraction (6,19,21,24). Contado *et al*.(19,24) used a mixture of three solvents and ultrasound followed by a phase separation to extracts nanoparticles from one sunscreen prior to flow field flow fractionation. The extracted particles were 50-200 nm large and maximal recoveries were below 25%. Lewicka and Goenaga-Infante (6,24) used chloroform and centrifugation to extract nanoparticles from 8 sunscreens and characterize their size, composition and crystalline phase but did not provide recovery or surface characterization. Nischwitz *et al*. (21,24) compared two methods using a methanol-water mixture and/or hexane and sonication to disperse sunscreens before decantation or centrifugation of the particles. Extraction using hexane was shown to be more efficient and could recover primary particles and recoveries were 68-110%. Addition of hexane was required to stabilize the final nanoparticle suspensions. Particle sizes determined using flow field flow fractionation were between 15-40 nm. Bairi *et al*. (24) extracted TiO_2 and ZnO from eleven sunscreens using tetrahydrofuran and determined their size and crystallinity, recovery and surface characterization were not reported. In all reported studies, agglomeration after extraction was a challenge for the characterization of the particles in suspension.

However, organic solvents may alter particle coatings. For instance, polydimethylsiloxane can be dissolved in hexane, tetrahydrofuran and hexane, especially during ultrasonication (25). Furthermore, organic solvents must be removed prior to biological exposure due to their negative biological effects. This is highly important when the extracted particles should be used for ecotoxicity test or mesocosm experiments, for instance. However, the published studies on extraction techniques did not focus on the further use of the extracted TiO_2 nanoparticles in environmental studies which require a large quantity of particles and a minimal alteration of the particle characteristics. Thus, a dedicated method is needed for extracting nanoparticles form sunscreens without using organic solvents, acid digestion, oxidative agents or ultrasonication.

Therefore, this study aimed at evaluating an extraction method for TiO_2 nanoparticles directly from sunscreens with minimal modifications of particle characteristics and test whether the extraction can be applied for the extraction of several grams of TiO_2. The method was evaluated for its recovery and purification efficiency. In addition, all extracted nanoparticles were characterized for their size, shape, surface charge, coating, and stability towards aggregation in the extraction medium.

Material and methods

Sunscreens

Eleven commercially available sunscreen products with differing sun protection factor (SPF), texture (lotion or cream), and specificities (dedicated to infants, sensitive skins or biological, for instance) were purchased at local shops (Rewe, Real, Müller, and DM) in Landau in der Pfalz (Germany) and on the internet (sebamed.com) in 2012. This selection is representative of the variety of sunscreen products used in Germany. Relevant information provided on the packaging for the sunscreen samples used in this study as well as their reference number is shown in **table 1** and the detailed ingredients list can be found in the supporting materials. In this report, sunscreen samples will be denoted by SX, where X is the number of the respective sunscreen given in the **table 1**. TiO_2 was the main inorganic component of these sunscreens, except for S10, which contained ZnO as main component. SiO_2 and Al_2O_3 were mentioned as minor ingredients in several sunscreens. Sunscreen bottles were vigorously shaken before opening. A small portion of the sunscreen was pushed out of the bottle and discarded and the rest of the sample was processed further.

Table 1: Selected information about the sunscreens used in this study and based on their respective packaging.

Number	Trade Name	Type	Specification	SPF	TiO_2	ZnO	SiO_2	Al_2O_3
1	Rewe Feuchtigkeits-Sonnenspray	Lotion	For sensitive skin	30	yes	no	no	no
2	Rewe Feuchtigkeits-Sonnencreme	Cream	For children	50	yes	no	no	no
3	Real,-Quality Sonnenmilch	Lotion	Refreshing	30	yes	no	yes	no
4	Real,- Quality Sonnencreme	Cream	Anti-aging	30	yes	no	no	no
5	Biotherm Lait Solaire	Lotion	–	50	yes	no	no	no
6	Nivea Sun Pflegende Sonnenmilch	Lotion	Refreshing	50	yes	no	no	no
7	Sundance Sonnenmilch	Lotion	Antiradical	50	yes	no	yes	no
8	Garnier Ambre Solaire Resisto Sonnenschutz-Milch	Lotion	For children	50	yes	no	yes	no
9	Alverde Sonnencreme Jojoba	Cream	For sensitive skin	30	yes	no	no	yes
10	Babylove Sonnencreme	Cream	For infants	50	yes	yes	no	no
11	Baby sebamed Sonnenschutzlotion	Lotion	For infants	50	yes	no	yes	no

Extraction methods

For S1-7, the following method was applied: 50 mg of sunscreen and 10 mL of 0.1 % Triton X-100 (Alfa Aesar, Germany) aqueous solution with a pH adjusted to 12 with NaOH (p.a., Sigma-Aldrich, Germany), were stirred in a glass beaker until a homogeneous suspension was obtained (30 min). The milky suspension was transferred to ultrafiltration units (Amicon Ultra-15 Centrifugal Filter Tubes, Millipore, Merck, Germany; cut-off: 30 kDa) and centrifuged at 4 500 r.p.m for 30 min using a centrifuge Universal 320 from Hettich Zentrifugen, Germany. Filtrate from the tube was discarded and the concentrate was redispersed in 10 mL of the Triton X-100 solution. In total, the filtration and resuspensions steps were repeated three times.

As S8-11 were not completely dispersed in the surfactant solution, a more lipophilic solvent: *n*-hexane (Rotisolv HPLC, Carl Roth, Germany) had to be used instead of Triton X-100 aqueous solution for the first dispersion step. The sunscreen suspended in *n*-hexane was centrifuged in glass tubes at 5 000 r.p.m. for 20 min. *n*-hexane supernatant was removed using Pasteur pipette and the remaining *n*-hexane was evaporated under the fume hood. The residue was redispersed in a 0.1 % Triton X-100 solution (pH = 12), sonicated for 15 min, transferred

123 to ultrafiltration unit and centrifuged at 4 500 r.p.m. for 30 min. Two further ultrafiltration steps were carried out
124 as for S1-7. The sonication step is optional and is for accelerating the dispersion step only.
125 For isoelectric point and time-of-flight secondary ion mass spectrometry (ToF-SIMS) measurements, three
126 additional ultrafiltration and redispersion steps were performed using pure water instead of Triton X-100
127 solution. This additional purification was required to reduce the pH of the solution and the surfactant
128 concentration since a high initial pH would have required the addition of a high amount of acid for the titration
129 during isoelectric point determination, whereas the presence of surfactant results in a high background in
130 ToF-SIMS.
131 S1, S2, S5, and S6 were chosen as a representative set of sunscreens for testing an extraction procedure on a
132 larger scale. Using ultracentrifugation instead of ultrafiltration allowed separating larger volumes at once. 0.5 g
133 of sunscreen and 200 mL of 0.1 % Triton X-100 solution with pH = 12 were stirred and homogenized as
134 previously described. The suspension was transferred to one 250 mL ultracentrifuge tube made of PTFE, bath
135 sonicated for 15 min in an ultrasonic cleaner (VWR, USA) and centrifuged at 20 000 r.p.m. for 30 min using a
136 WX Ultra Series Centrifuge from Thermo Scientific, Germany. The supernatant was carefully removed by
137 Pasteur pipette and the solid residue was redispersed using 200 mL of Triton X-100 solution. The
138 ultracentrifugation step was repeated three times in total. For S8 and S11, the same procedure was followed for
139 larger scale extraction with *n*-hexane for the first extraction step instead of Triton X-100 solution. All extraction
140 samples were done in triplicates.
141
142 *Digestion procedure for determination of total Ti content*
143 In a 15 mL glass beaker, 5 mL of hydrogen peroxide (30 %, Rotipuran®, Carl Roth, Germany) were added to
144 50 mg of sunscreen and let stand for 10 min before 10 mL of sulfuric acid (95 %, Rotipuran®, Carl Roth,
145 Germany) were then added dropwise to the mixture. After standing for 15 min, the beaker was covered by a
146 watch glass and progressively heated until a strong ebullition was observed (approximately at 225°C). After one
147 hour of ebullition, the mixture was cooled to room temperature, quantitatively transferred into a 100 mL
148 volumetric flask and diluted with ultrapure water (resistivity 18.2 MΩ·cm, Reinstwassersystem EASYpure II™,
149 Werner, Germany). A sample of this solution was further diluted in pure water prior to ICP-MS analysis. For
150 TiO_2 particle suspensions, 10 mL of undiluted suspension was dried at 95 °C in a beaker before following the
151 same digestion procedure as for sunscreens.
152 A X-Series 2 system (Thermo, Germany) was used for ICP-MS measurements. The system was equipped with a
153 quadrupole mass spectrometer, a platinum sample cone, a PTFE spray chamber thermostated with a Peltier

cooler and an autosampler equipped with a FAST system (ESI, Germany). The isotopes ^{46}Ti and ^{47}Ti were monitored as strong interferences from the diluted digestion media were observed with other isotopes. A rhodium solution (Peak Performance, California, USA) was used as an internal standard. Calibration was carried out using TiO_2 (P-25, Degussa, Germany) particles, which were digested following the same procedure than used for the samples. The recovery of the method was determined using standard addition in S5 and was 95 %. No significant matrix effect could be observed from the sunscreen (see supporting materials for more details).

Determination of 1-(4-Methoxyphenyl)-3-(4-tert-butylphenyl)propane-1,3-dione (avobenzone) concentration

Avobenzone concentration in the sunscreen and in the supernatant of the extracted suspension was measured as an indicator of the purification efficiency of the extraction method using ultracentrifugation.

For the sunscreen extracts: 5 mL of the sunscreen extracts were ultracentrifuged for 35 minutes at 50 000 rpm in order to remove the particulate fraction. Calculations based on technical data provided by the ultracentrifuge manufacturer showed that spherical 5 nm TiO_2 nanoparticles would sediment from the top to the bottom of the tube in 27 min under those conditions. 2 mL of the supernatant were mixed with 1 mL of acetonitrile (>99.9%, HPLC grade, Sigma Aldrich, Germany) and transferred to a quartz cuvette for UV-absorbance measurements.

For the first supernatant: sunscreens were suspended as described above. S1-7 were centrifuged at 50000 r.p.m for 30 minutes and 0.1 mL of the supernatant were diluted in 5 mL of a 1:2 acetonitrile-Triton X-100 extraction solution mixture and transferred to a quartz cuvette for UV-absorbance measurements. S8-11 were centrifuged in glass tubes at 5000 r.p.m. for 20 minutes. 0.1 mL of the supernatant were evaporated and diluted in in 5 mL of the 1:2 acetonitrile-Triton X-100 mixture and transferred to a quartz cuvette for UV-absorbance measurements.

UV-absorbance were measured using a Specord50 spectrometer (Analytik Jena, Germany) at the wavelength of 355 nm (absorbance peak of avobenzone) and with an integration time of 2 s. UV measurements were repeated five times. Calibrants were prepared in the same eluent than the nanoparticle suspension using pure avobenzone (Fluka, pharmaceutical secondary standard, Germany).

Transmission Electron Microscopy (TEM)

Undiluted dispersions of nanoparticle suspensions were nebulized using an ultrasonic generator (proprietary system developed at the Karlsruhe Institute of Technology) onto a 3 mm copper grid covered with a combined holey and ultrathin carbon film (Ted Pella, Inc., Redding, USA). Measurements were done using a Leo 912 OMEGA TEM (Carl Zeiss, Germany). Images were acquired at beam intensity of 120 kV and magnification of

20 000×. For each sample, approximately 10 images were acquired in order to obtain more than 200 measurable particles. Obtained images were analyzed for size and shape manually using the software ImageJ.

Cryogenic Transmission Electron Microscopy (cryo-TEM)

A drop of sunscreen was deposited on a "Quantifoil"® (Quantifoil Micro Tools GmbH, Germany) carbon membrane. The excess of sunscreen on the membrane was absorbed with a filter paper and the membrane was quickly quench-frozen in liquid ethane to form a thin vitreous ice film. Once placed in a Gatan 626 cryo-holder cooled with liquid nitrogen, the samples were transferred in the microscope and observed at low temperature (-180 °C). Cryo-TEM images were recorded on an ultrascan 2k CCD camera (Gatan, USA), using a LaB_6 JEOL JEM2100 (JEOL, Japan) cryogenic microscope operating at 200 kV with a JEOL low dose system (Minimum Dose System, MDS) to protect the thin ice film from any irradiation before imaging and to reduce the irradiation during the image capture. Particle elemental composition was analyzed using an X-ray energy dispersive spectroscopy (XEDS) detector mounted on the microscope (JEOL Si(Li); resolution: 140 eV). XEDS analyses were always carried out in regions where particles were on the carbon film since ice can melt in holes of the carbon film during spectra acquisition.

Dynamic light scattering

Two milliliters of particle suspension diluted 1:200 with 0.1 % Triton X-100 solution at a pH value of 12 were transferred into polystyrene cuvettes, bath sonicated for 15 min, and analyzed with a Delsa™ Nano C particle analyzer (Beckman Coulter, USA) using a laser with a wavelength of 658 nm and at a scattering angle of 165°. A CONTIN algorithm was used for calculating the particle size distribution from the autocorrelation function. The accumulation time was 60 s and each measurement was triplicated. Instrument performance was verified using standard polystyrene nanoparticles supplied by the instrument manufacturer. Dilution and sonication time were optimized for obtaining reproducible results, even with unstable suspensions (for details see **SI-tables 2-3**). Stability of extracted particles in terms of size was investigated by measuring the hydrodynamic diameter of extracted particles with DLS directly after the extraction and after two weeks kept at room temperature.

Isoelectric point

The extracted particle suspension in pure water was sonicated for 5 min and 1 mL was sampled and diluted in 10 mL of a solution containing 0.1 % Triton X-100 (Alfa Aesar, Germany) and 10 mM NaCl (p.a., Roth, Germany). ζ-potential measurements of the surfactant solution without sample confirmed that possible micelles did not

affect the ζ-potential measurements. The addition of surfactant aimed at reducing the size of agglomerates, thus improving the accuracy of ζ-potential measurements. The diluted suspension was sonicated for 5 min. The final pH values of the suspensions were between 5-6. The suspension was transferred to a 50 mL polypropylene tube which was positioned in an MPT-2 autotitrator (Malvern Instruments, Germany) connected to a Zetasizer Nano ZS light scattering apparatus (Malvern Instruments, Germany) equipped with a folded capillary cell. The pH was adjusted using the autotitrator with 0.25 M or 0.025 M HCl (Rotipuran, Roth, Germany) and 0.25 M NaOH (puriss. p.a., Sigma-Aldrich, Germany) solutions by decreasing the pH from the initial pH to approximately 1.6 with an increment of 1 (tolerance of 0.4). For each pH value, three ζ-potential measurements (30 data points per measurements) were performed. The Smoluchowski approximation was used for converting electrophoretic mobility values into ζ-potential. The sample cell was recirculated after each measurement. Isoelectric point determination was repeated two times for each sunscreen extract.

Time-of flight secondary ion mass spectrometry (ToF-SIMS)

A ToF.SIMS5 instrument (ION-TOF GmbH, Münster, Germany) equipped with a Bi cluster primary ion source and a reflectron type time-of-flight analyzer was used for ToF-SIMS measurements. Base pressure was lower than 5×10^{-9} mbar. For high mass resolution, the Bi source was operated in the "high current bunched" mode providing short Bi_3^+ primary ion pulses at 25 keV energy, a lateral resolution of approximately 4 µm, a target current of 0.25 pA at a repetition rate of 4.4 kHz. The short pulse length of 1.1 ns allowed for high mass resolution. Two measurements were performed for each sample consisting of an air-dried droplet of all sunscreen extracts deposited onto a gold coated silicon wafer:

- Static SIMS analysis to determine the surface compositions: the primary ion beam was rastered across a 500×500 µm^2 field of view on the sample, and 128×128 data points were recorded. Primary ion doses were kept below 10^{11} ions cm^{-2} (static SIMS limit). Spectra were calibrated on the omnipresent C^-, C_2^-, C_3^-, or on the C^+, CH^+, CH_2^+, and CH_3^+ peaks. Based on these datasets the chemical assignments for characteristic fragments were determined.
- Surface erosion / depth profiling with an argon cluster beam to reduce surface contaminations and organic layers on the inorganic nanoparticles. Hereto, a dual beam analysis was performed in non-interlaced mode: the primary ion source was again operated in "high current bunched" mode with a scanned area of 200 × 200 µm^2 (4 frames with 64 × 64 data points) and a sputter gun (operated with Ar_{1200}^+ ions, 2.5 keV, scanned over a concentric field of 400 × 400 µm^2, target current 0.9 nA) was applied to erode the sample for 4 scans (6 s) followed by a 0.5 s pause to reduce surface charging from the sputter process. Argon cluster ions are

eroding the softer organic layers faster as compared to the harder mineral particles underneath. The total sputter time was set to 500 s corresponding to a sputter dose of 1.75×10^{15} ions cm^{-2}. Presented spectra are integrated over time.

Results and discussion

Extraction procedure: method development

The dispersion of sunscreens had to be optimized prior to separation using ultrafiltration or ultracentrifugation. Several aqueous and non-aqueous solvents were tested for their ability to disperse sunscreens at room temperature without using ultrasonication. 1 % (w/w) aqueous solutions of sodium dodecyl sulfate (SDS), Brij L35 and Triton X-100 surfactants and *n*-hexane were tested to investigate the ability to suspend each of the sunscreen samples. Triton X-100 solution was the most efficient aqueous dispersant for all tested sunscreens based on visual aspect of the suspension after 30 min stirring. Pictures of suspensions obtained after 30 min stirring can be found in the supporting information (SI-figure 1). The efficiency of the suspension step varied from one sunscreen to the other. While S1-7 formed homogeneous suspensions in aqueous solutions and were not dispersed in *n*-hexane, S8-11 were not completely suspended in aqueous solvents, whereas a milky suspension was obtained with *n*-hexane. Therefore, Triton X-100 solution was selected for dispersing S1-7. For S8-11, *n*-hexane was used for the first dispersion step in order to obtain a complete dispersion. After a first centrifugation step, the remaining pellets could be easily dispersed in the Triton X-100 solution for further purification. Thus, this method minimizes the use of *n*-hexane but ensures a complete dispersion of the sunscreen and made possible to use ultrafiltration membranes, which are not compatible with organic solvents, for further purification.

As concentrated surfactant solutions can damage ultrafiltration membranes (information from the supplier), lower Triton X-100 concentrations were tested. A concentration of 0.1 % was chosen as it was harmless for the ultrafiltration membrane and could completely dispersed S1-7 (SI-Figure 1). In addition, neutral (without acid or base addition), acidic (pH = 2, HCl), and basic (pH = 12, NaOH) Triton X-100 solutions were tested. The basic solution was the most efficient dispersant for sunscreen and extracted particles based on visual aspect (SI-Figure 1). Most probably, hydroxide ions can induce the partial hydrolysis of ester groups presents in several sunscreens major components (e.g. octocrylene, alkyl benzoates, 2-ethylhexyl salicylate) resulting in more hydrophilic products and, therefore, in more efficient dispersion of the sunscreen. Therefore, a basic solution of 0.1% Triton X-100 was used to disperse and purify the sunscreens tested in this study.

Ultrafiltration is advantageous for extracting lower amounts (15 mL per tube in this study) of sunscreens as the cut-off is more accurate and depends mainly on the geometrical size of the molecules or particles to be retained, whereas ultracentrifugation separates particles based on their size and density. On the other side, the cut-off of ultracentrifugation can be adapted by changing the rotation speed. In addition, this technique was more adapted for separating large amounts of dispersed sunscreen. Therefore, a larger scale separation method using 250 mL ultracentrifugation tubes was tested. This method allowed preparing 1 L of final isolated TiO_2 nanoparticles suspension (approximately 250 mg L^{-1}, based on average final concentrations obtained in this study) can be prepared in one working day. This is an improvement compared to a recently reported extraction method (21,24) in which tetrahydrofuran was used as a solvent, since the reported procedure took more than one day to be completed. The absence of organic solvent in the final suspension and of ultrasonic treatments are advantages of the method evaluated in this study compared to other previously reported methods (19,21).

Recovery and purification efficiency determination

Average total TiO_2 concentrations were determined using ICP-MS after sunscreen digestion in a mixture of sulfuric acid and hydrogen peroxide. This method has the advantage of being simple and avoiding using HF, while dissolving all sunscreen components including TiO_2. We assumed that all detected Ti was particulate TiO_2. This assumption is reasonable considering the information provided by the sunscreen suppliers and Ti chemistry (26). Total TiO_2 concentrations were in the range of 4-6% (w/w) except for S9 which has a concentration of 13% (w/w) (**table 2**). These values are in the range of expected concentrations in sunscreens and similar to values reported elsewhere (19). TiO_2 concentrations of the purified suspensions were between 200-350 mg L^{-1} (**table 2**). Recoveries in terms of TiO_2 particles were determined by dividing the TiO_2 concentrations in extracted particles suspensions by the TiO_2 concentration in the sunscreen and ranged between 72-98% for all methods and samples except for S9 with a value near 51% (**table 2**). Considering TiO_2 content and recovery, S9 seems to be an exception. The producer claimed that this sunscreen contained mainly plant extracts and TiO_2. Therefore, the matrix of this sunscreen strongly differed from the rest of the tested sunscreens. Nonetheless, recoveries are overall highly satisfying, since they are comparable to recoveries obtained by Nischwitz *et al.* (64-110%)(21). Recoveries for the methods using ultracentrifugation and ultrafiltration were comparable.

Table 2: total TiO_2 contents in sunscreens and concentrations of TiO_2 particles in the suspensions obtained after extraction from sunscreens using ultrafiltration (10 mL of purified suspension: small scale) or ultracentrifugation (200 mL of purified suspension: large scale) and the corresponding extraction efficiencies. Ti concentrations were determined using ICP-MS. The given errors denote the standard deviation determined using values from three replicated extractions. The stars on the sunscreen numbers indicate that these sunscreens were extracted using *n*-hexane instead of Triton-X 100 solution for the first purification step.

N°	TiO_2 content in sunscreens (% (w/w))	TiO_2 concentration ultrafiltration (mg L^{-1})	Recovery (%)	TiO_2 concentration ultracentrifugation (mg L^{-1})	Recovery (%)
1	4.1 ± 0.3	231 ± 31	96.0 ± 7.2	240 ± 17	90.6 ± 5.3
2	6.1 ± 0.7	256 ± 19	73.2 ± 6.7	375 ± 31	94.4 ± 9.2
3	5.5 ± 0.4	272 ± 17	88.2 ± 8.6		
4	4.0 ± 0.5	210 ± 20	83.0 ± 7.4		
5	4.1 ± 0.2	209 ± 21	87.3 ± 6.0	213 ± 26	94.5 ± 7.6
6	5.2 ± 0.8	281 ± 24	88.2 ± 7.8	212 ± 12	78.0 ± 4.0
7	6.0 ± 0.9	312 ± 37	73.7 ± 12.3		
8*	5.5 ± 0.1	272 ± 10	95.7 ± 2.3	270 ± 33	98.0 ± 6.2
9*	13.1 ± 0.7	342 ± 9	51.7 ± 5.6		
10*	5.9 ± 0.2	251 ± 11	83.5 ± 7.9		
11*	6.4 ± 0.5	239 ± 25	72.8 ± 6.3	308 ± 27	98.2 ± 5.4

For ultrafiltration, the final volume of the particulate fraction in the concentrate can be controlled by setting the time or the speed of the centrifugation step. Therefore, the concentration of the non-particulate compounds relative to TiO_2 would be decreased by a factor of 1000-6000 after three successive filtration steps considering the final volume of the concentrates (0.5-1 mL for our samples).

A similar estimation of purification rate could not be achieved for ultracentrifugation, since the removal of the supernatant was difficult to reproduce. Indeed, pellets were not observed for all samples tested in this study after ultracentrifugation. Thus, the volume of the removed supernatant had to be adapted for each sample. Therefore, the efficiency of the ultracentrifugation technique in terms of removal of the molecular matrix was tested in order to quantify the variation of the purification efficiency for different samples. This can be achieved by determining the concentration of the non-particulate fraction before and after purification by ultracentrifugation.

As sunscreen compositions are diverse and complex, a systematic measurement of all compounds in the suspension of extracted TiO_2 would be especially tedious and inefficient. Therefore, we used 1-(4-Methoxyphenyl)-3-(4-*tert*-butylphenyl)propane-1,3-dione (avobenzone), as a representative of the non-

particulate fraction. Avobenzone was selected because it is a widely used UV-A blocker and was one of the main ingredient in all tested sunscreens except S9 and S10. In addition, avobenzone has an absorption peak at 355 nm which renders possible a selective quantification in the presence of Triton-X (absorption peak at 280 nm) using UV-spectrometry. We assumed that avobenzone was the only compound absorbing at that wavelength in our sunscreen extracts despite the possible interferences of other organic UV blockers in the sunscreens such as octocrylene (absorbance peak at 305 nm). This an acceptable working hypothesis since the determination of absolute concentration of avobenzone was not required for determining the purification rate.

The concentrations of avobenzone in the sunscreen extract were between 0.1 and 25.1 mg L^{-1} (**table 3**) and were, therefore, much lower than the concentrations measured in the first supernatant (before the first centrifugation step). In this study, we defined the purification rate as the ratio between the TiO_2/Avobenzone mass to mass ratio calculated in the first supernatant and the TiO_2/Avobenzone ratio in the final TiO_2 extracts. Purification rates ranged from approximately 8 to 2002 (**table 3**). In other words, the concentration of avobenzone relative to TiO_2 was divided by 8 to 2002 after purification. This values can be compared to the purification efficiency determined for S11 using the ultrafiltration method (**table 3**) which were 5417 and, thus, in the range of the efficiency estimated from the remaining volume after filtration (see above).

The complexity of the matrix and the multiple possible interactions between the various dissolved compounds (e.g. sorption, macromolecular assemblies) during the centrifugation process could explain the differences observed between the sunscreen extracts. The observed variations between samples in terms of purification efficiency indicates that great care has to be taken when using ultracentrifugation for purifying nanoparticles extracted from complex mixtures. We also recommend to, at least, estimate the purification rate for applying this method to further sunscreens. It has to be noted that it is always possible to increase the purity of the nanoparticle extracts by carrying out further purification steps, if the target experiments require a high purity.

Table 3: Avobenzone concentrations in the first supernatant and after purification using ultracentrifugation measured by UV-spectrometry performed after removing the particulate fraction. Standard deviations were determined from 5 replicates. The given purification rate is here defined as the ratio between the TiO_2/Avobenzone mass to mass ratio calculated in the first supernatant and the TiO_2/Avobenzone ratio in the final TiO_2 extracts. The asterisk denotes the results obtained for ultrafiltration for comparison purposes.

Sunscreen N°	Avobenzone concentration in the first supernatant in mg L^{-1}	Avobenzone concentration in the final extract in mg L^{-1}	Purification rate
1	282.4 ± 0.2	0.16 ± 0.01	2002
2	165.0 ± 0.4	25.09 ± 0.06	8
5	117.1 ± 0.2	1.63 ± 0.01	76
6	145.5 ± 0.3	1.86 ± 0.01	60
8	268.3 ± 0.7	8.37 ± 0.01	32
11	338.6 ± 0.4	0.24 ± 0.01	1420
11*	338.6 ± 0.4	0.049 ± 0.007	5417

Characterization of particles in sunscreen

In order to evaluate possible modifications of particles structure induced by the extraction process, nanoparticle imaging inside four sunscreens with differing particle morphology and including one "lipophilic" sunscreen (which could not be dispersed in the Triton X-100 solution) was carried out. As TEM measurements require high vacuum and the main component of sunscreens is water, drying artefacts are expected to occur. Therefore, cryo-TEM was used to avoid drying artefacts by imaging the sample in the frozen state. The samples were cooled down to -180°C fast enough for allowing amorphous ice to form, thus, immobilizing instantaneously sunscreen constituents. Thus, we can exclude drying artefacts and observation of the actual particle structures and organization inside the sunscreens was facilitated.

TiO_2 particles used in sunscreens were very diverse. Two main types of shapes were observed: spherical, irregular, and elongated (**figure 1**). Energy dispersive X-ray spectroscopy confirmed that the particles contained Ti (**SI-figure 2**). Almost all particles observed were agglomerated in the sunscreens 1 and 7, whereas some isolated primary particles were observed in sunscreens 5 and 9. Nonetheless, most of the observed particles were agglomerated. Therefore, we can assume that most of the nanoparticles present in the sunscreen were agglomerated prior to extraction.

Interestingly, TiO_2 nanoparticles were frequently observed agglomerated on large (several hundreds of nanometers) spherical particles (**figure 1**). The weak contrast compared to the water background suggests that

these particles were composed of organic materials. We suppose that these spherical objects are organic components of the sunscreens in the form of emulsion in water. As the water is frozen, these lipophilic drops would be trapped in the ice matrix (27). The fact that TiO_2 nanoparticles were often attached on their surfaces suggests that their coating is lipophilic. Cryo-TEM images suggest a high concentration (especially in S5 and S9) of these organic particles in the sunscreen. Therefore, we can exclude that these particles are hard polymer sphere, since they would be concentrated with the inorganic particles during ultrafiltration. In fact, this is not reflected by the TEM and DLS analyses of the extracted fractions (see below). Indeed, cryo-TEM pictures suggest a high concentration of these organic particles in the sunscreens, especially in 5 and 9 (**figure 1**), which should strongly influence the DLS results and being observable in classical TEM.

Characterization of the extracted particles

The size and the shape of TiO_2 particles extracted from sunscreens were determined using classical TEM and DLS. On the TEM pictures particles appear strongly agglomerated due to the drying of the suspension (**figure 2 and SI-figure 3**). Agglomeration due to drying effects using classical TEM was not of concern, since the shape and the size were determined for the primary particles only. The same shape variety of the primary particles as in the cryo-TEM pictures was observed with irregular, angular (e.g. triangular, rectangular), spherical, ellipsoidal or elongated particles. While some S2, S4, S5, and S8 were homogeneous in terms of shape, S7 and S9-11 were highly heterogeneous. Some similarities were found in the particle shape and size between different sunscreens suggesting that particles of different types were mixed on purpose in some sunscreens. Shape and size of extracted nanoparticles was conserved after extraction as shown by comparing pictures from cryo-TEM and TEM experiments. Therefore, we can assume that there is no other structure disruption due to the extraction process, except disagglomeration. Disagglomeration was obvious when comparing average hydrodynamic diameter measured in the sunscreen extracts suspensions using DLS with the size of agglomerates in the sunscreen before extraction observed with cryo-TEM (**table 4**).

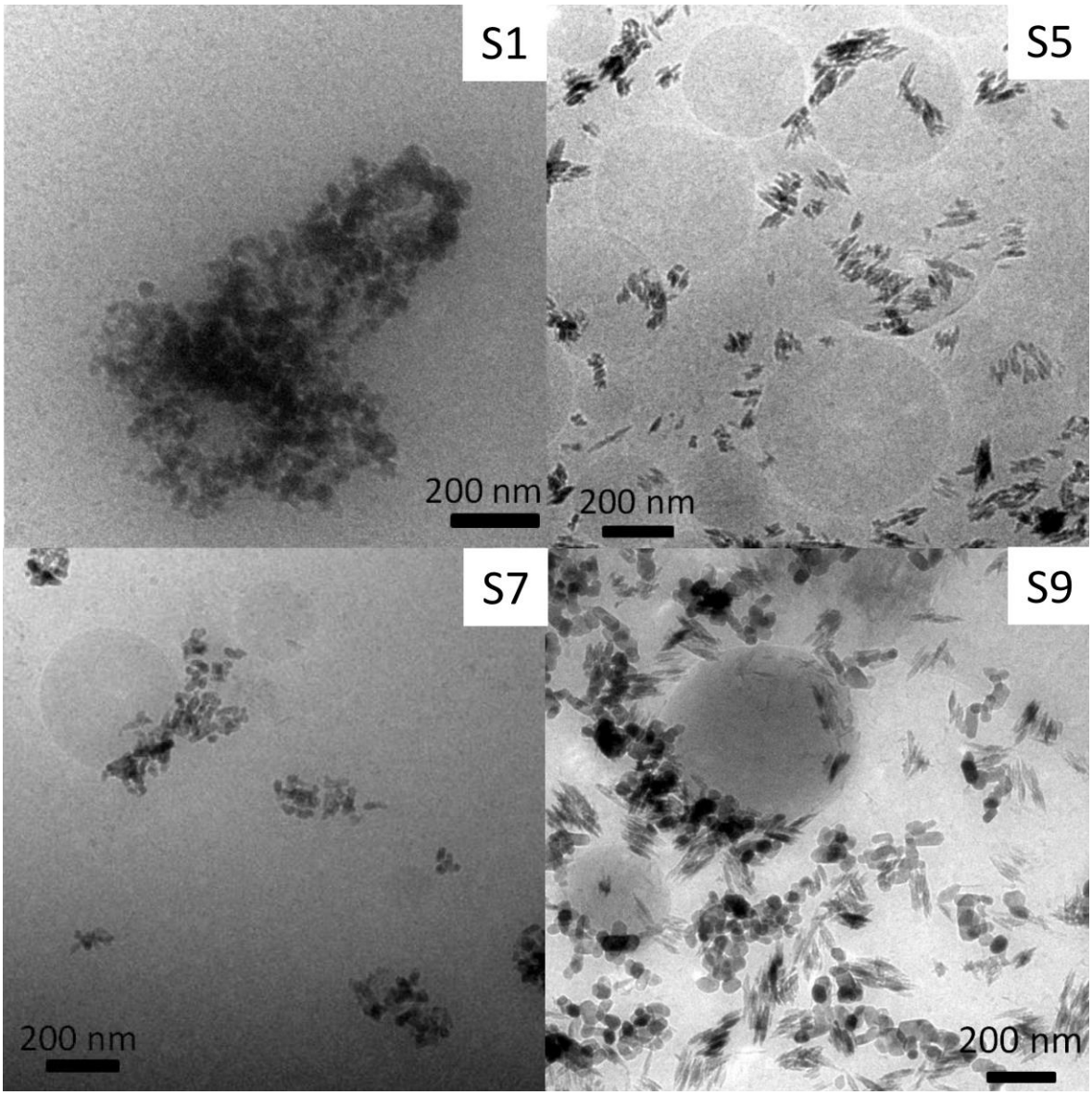

Figure 1: Representative images of TiO_2 particles in sunscreens obtained using transmission electron microscopy in cryogenic mode. The sunscreen number is given on the upper right corner.

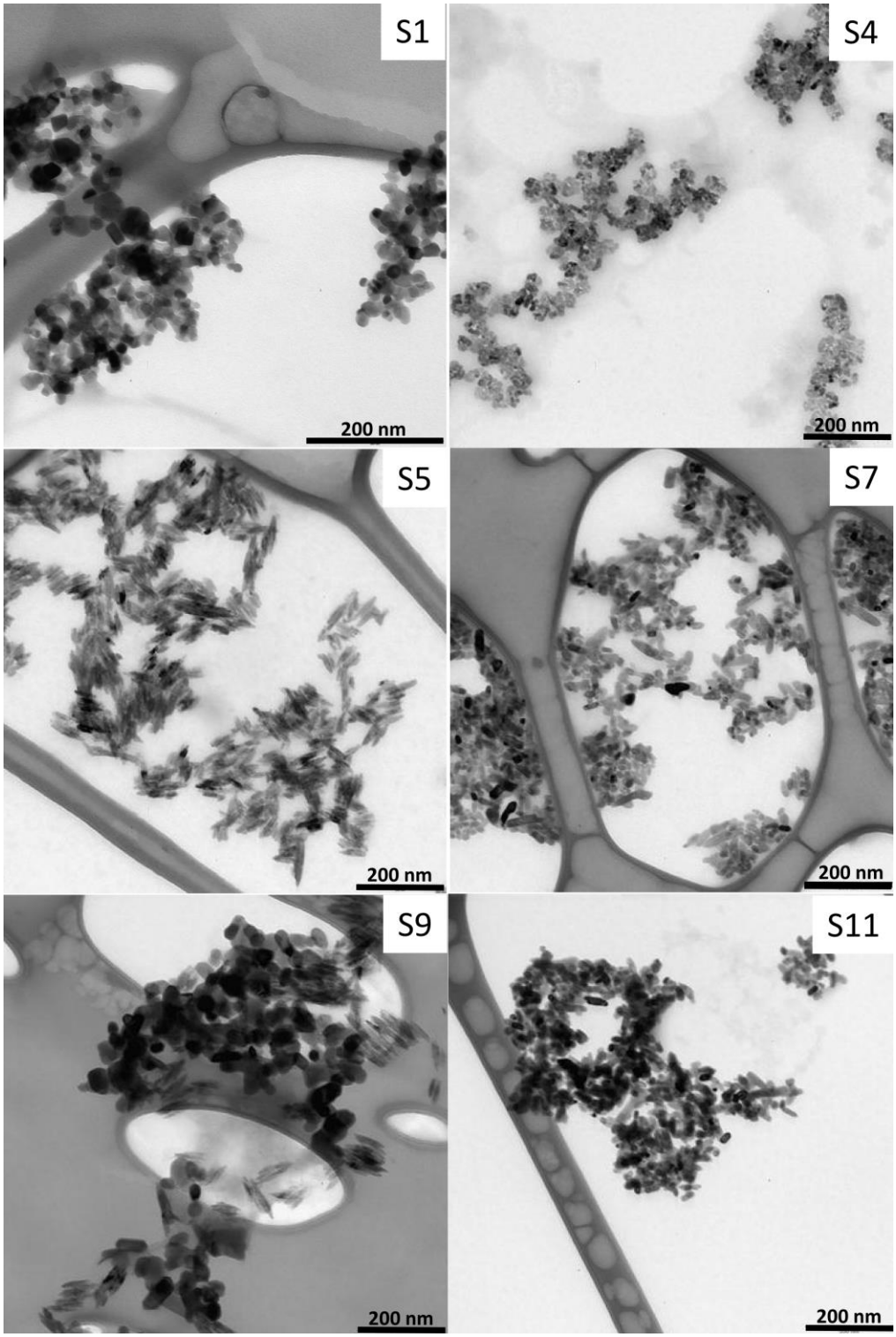

Figure 2: Representative images of extracted inorganic nanoparticles from eleven commercial sunscreens obtained using transmission electron microscopy. The sunscreen number is written on the upper right corner. TEM pictures of the other sunscreens extract can be found in the supporting information (SI-figure 3). TEM images from S2, S6, and S10 and were similar to S1, whereas images from S3 and S8 were similar to S7 and S5, respectively.

Table 4: Arithmetic mean size parameters and shape description of extracted nanoparticles measured using TEM, average hydrodynamic diameter measured using DLS, isoelectric point determined from acid titration and electrophoretic mobility measurements, and surface coating as suggested by ToF-SIMS results and by information on the formulation. The mean parameters measured with TEM correspond to the size of more than 200 primary particles for each sample. Length denotes here the longest distance between two points belonging to the particle, whereas widths denotes the corresponding shortest distance. TEM values are given with the standard deviation of the corresponding size distribution. DLS values are given with the standard deviation determined from three measurement replicates. Isoelectric points were determined using values from two titrations for each sample. PDMS: polydimethylsiloxane.

N°	Average length (nm)	Average width (nm)	Particle shape	Average hydrodynamic diameter (nm)	Isoelectric point	Proposed surface coating
1	19.9 ± 6.7	14.2 ± 5.0	spherical, irregular	23.2 ± 1.2	2.6	PDMS
2	23.4 ± 7.2	15.0 ± 4.8	spherical and angular	28.0 ± 1.0	2.2	PDMS
3	35.5 ± 12.0	15.9 ± 3.9	ellipsoidal and angular	35.5 ± 2.0	1.7	PDMS
4	13.4 ± 3.1	7.5 ± 1.7	spherical	19.3 ± 0.8	1.9	PDMS
5	36.6 ± 11.6	7.3 ± 2.5	elongated	24.8 ± 0.8	1.9	PDMS
6	24.2 ± 6.6	15.0 ± 4.3	spherical	34.3 ± 0.6	< 1.8	SiO_2
7	32.5 ± 12.1	13.9 ± 3.7	ellipsoidal	30.8 ± 1.0	< 1.8	PDMS
8	29.3 ± 10.0	9.3 ± 3.7	elongated, spherical and ellipsoidal	22.3 ± 0.8	2.1	PDMS
9	42.0 ± 12.5	22.7 ± 7.5	spherical, angular and elongated	35.6 ± 0.6	4.5	Al_2O_3
10	48.8 ± 16.6	31.5 ± 12.6	spherical	37.6 ± 1.5	4.4	$Al(OH)_3$
11	27.0 ± 11.4	12.4 ± 3.9	ellipsoidal and spherical	27.4 ± 1.7	3.1	$Al_2O_3 + SiO_2$

The range of average primary particle sizes determined from TEM pictures was surprisingly narrow (length: 20-50 nm, width: 7-32 nm, **table 4**). Furthermore, low standard deviations indicate that particles used in sunscreen are fairly monodisperse. It was not possible to image any coating at the surface of nanoparticles using TEM or HR-TEM due to the low contrast between the coating and the carbon from the grid and the thinness of the coating layer.

Average hydrodynamic diameter obtained using DLS after sonication and dilution were measured for all extracted sunscreens (**table 4**). Sonication time and dilution ratio were optimized for obtaining primary particle size and, thus, obtaining reproducible size measurements (**SI-table 2-3**). Despite particle shape differences, there

is a good correspondence between the sizes of primary particles determined using TEM and the average hydrodynamic diameter obtained using DLS. This indicates that the extracted particles were in the form of primary particles or small agglomerates after extraction and sonication. Thus, extracted particles are disagglomerated during the dispersion processes. If it is required to obtain agglomerated particles, it is still possible to replace the surfactant based solution with pure water by further ultracentrifugation of ultrafiltration steps and, hence, induce re-agglomeration of the particles if the agglomerated form is crucial for the targeted investigations. However, extracting the particles from sunscreens without modifying their original agglomeration structure is still challenging as it would imply to avoid introducing any shear forces or stabilizing agent, which would not result in the dispersion of most sunscreens.

Determination of the isoelectric points is a classical approach to qualitatively estimate the surface charge behavior of colloids in aqueous media (28). Furthermore, particles are expected to agglomerate faster at pH near the isoelectric point due the lack of electrostatic repulsion (29). Therefore, we determined isoelectric points by measuring ζ-potentials at several pH values. The complete ζ-potential-pH curves can be found in the supporting information (**SI-figure 4**), while the isoelectric points measured for each sunscreen are summarized in **table 4**. The presence of the surfactant in the solution could influence the absolute ζ-potential value by shifting the shear plane on the particle surface. However, the isoelectric point is not affected as Triton X-100 is a neutral surfactant and the formation of micelles did not affect the measurements as verified with a blank sample. While S9-11 had an isoelectric point between 3 and 4.5, other extracts had an isoelectric point lower than 3. Nanoparticle extracted from sunscreens were thus all negatively charged at pH > 4 in NaCl aqueous solution. ζ-potential at pH = 5 were varying between 0 and -30 mV (**SI-figure 4**). Thus, particle stability in terms of agglomeration in aqueous media can be expected to vary strongly depending on the sunscreen used.

ToF-SIMS measurements allowed a deeper insight into the nature of the nanoparticles' coating. It has to be noted that the most part of the surfactant present in the extraction media was removed before ToF-SIMS measurements since its high concentration would have resulted in a thick layer of surfactant over the particles and would have disturbed the surface analysis. Fragments characteristic for typical coating materials (Al^+, $SiOH^+$, Zn^+, polydimethylsilane (PDMS): $SiC_3H_9^+$ at 73.05 m/z, and $Si_2C_5H_{15}O^+$ at 147.08 m/z) used in sunscreens (7,9,30) and TiO^+ as a marker of the bulk material were monitored before and after sputtering with Ar clusters. Several Zr^+ isotopes signals were monitored in addition but were insignificant for all samples measured. A decrease in signal intensity for a given fragment during sputtering combined to an increase of TiO^+ signal intensity indicates that the observed fragment originates from the very surface layer, which is removed during sputtering (31). As an example, ToF-SIMS measurements for S1 (**figure 3**) are quite clear in that respect. The

454 TiO^+ signal intensity increased with sputtering, indicating an increased exposure of the bare TiO_2 surface. On the
455 other hand, signal intensity of characteristic PDMS fragments dramatically decreased during sputtering
456 suggesting the absence of PDMS in the deeper layers. Therefore, we can conclude that PDMS is most probably
457 present on the surface layer of the TiO_2 nanoparticles extracted from S1. In this case, the weak $SiOH^+$ signal
458 more probably originates from the fragmentation of PDMS than from an additional underlying silica based
459 coating layer as the $SiOH^+$ signal intensity decreased after sputtering. Signal intensities of others ions were not
460 significant (lower than for the blank sample).

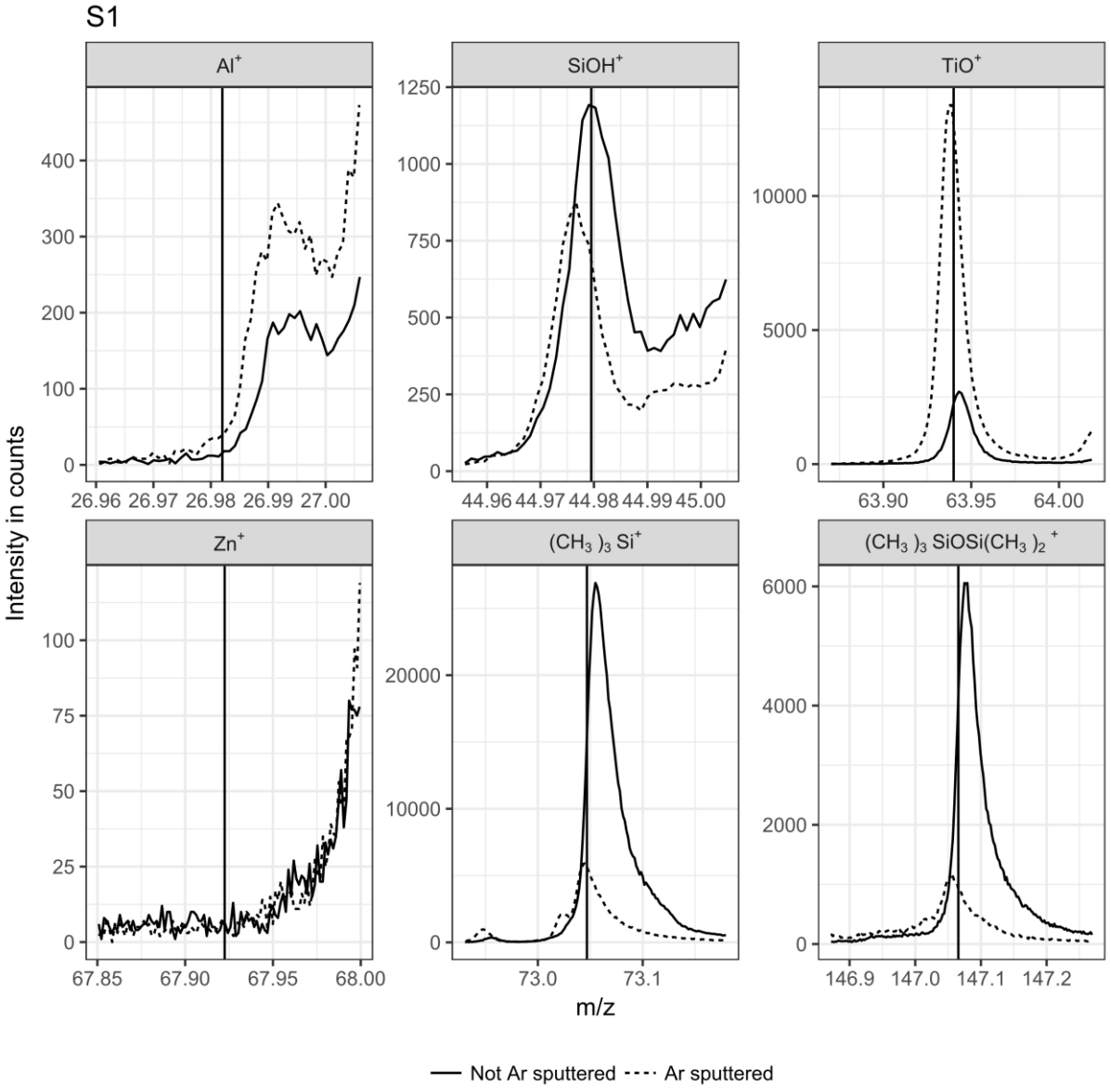

461

462 **Figure 3: ToF-SIMS signal intensities obtained without (full line) and with (dashed line) Ar-clusters**
463 **sputtering for S1. Vertical lines indicate the exact mass expected from the respective expected ions or**

fragments; from left to right: $^{27}Al^+$, $^{28}SiOH^+$, $^{48}TiO^+$, $^{68}Zn^+$, $(CH_3)_3Si^+$, and $(CH_3)_3SiOSi(CH_3)_2^+$. The two latter are characteristic fragments for PDMS (30)**.**

The other sunscreen extracts were analyzed following the same procedure (**SI-figure 5-15**). Absolute intensities for TiO^+ varied strongly between samples despite efforts made in selecting a scanned area completely covered with particles. This is probably due to visible differing topologies of the particle layer due to different agglomeration and deposition behavior during the drying process and to particle shape diversity. However, ToF-SIMS results from S1-5, S7, and S8 had similar patterns and may have, therefore, similar surface chemistry; except for S2 and S5, for which the PDMS signals were dominating. This can be explained by the presence of a PDMS layer thicker than other samples for which the surface coating was almost completely removed after the first erosion step. The erosion of a thick PDMS layer would take more time and, therefore, the signal integrated over time can become higher than the signal obtained from the first measurement (static SIMS). Therefore, we concluded that particles extracted from S1-5, S7, and S8 were most probably all coated with PDMS although with most likely differing coating thicknesses. Estimation of the coating thickness was not possible due to the above mentioned irregularities of the surface topology. Al^+ signals higher than the blank were observed for S5 and S8-11 indicating an Al-based coating such as Al_2O_3 or $Al(OH)_3$; in accordance with the formulation mentioning "alumina" for S10 and S11 and "aluminum hydroxide" for S5 and S10. No Al-containing compounds were mentioned in S8 and S11. However, the Al concentration in these sunscreens may be too low for being mentioned on the packaging as suggested by the weak Al^+ signals compared to TiO^+. As no other significant signals were observed for S9, we conclude that the nanoparticles are coated solely with Al_2O_3. Zn was detected in S10 and S11. This was expected for S10 since it contains ZnO nanoparticles in addition to TiO_2 nanoparticles. It has to be noted that, due to the presence of two types of nanoparticles in S10, it should remain undecided to which type the observed alumina coating belongs. Zn signal from S11 most probably results from residual sorption of Zn^{2+} ions on the TiO_2 nanoparticles from "Zinc stearate" present in the formulation. $SiOH^+$ was significant for S6 and S11, which is noticeable because the PDMS signals were weak for both samples. This suggests the presence of a silica based coating. Since amorphous SiO_2 could be partly dissolved under alkaline condition (pH > 10) (32), it cannot be completely excluded that S9 and S11 originally contained SiO_2 as a surface coating. The types of coating which are expected from the ToF-SIMS measurements are summarized in the **table 4**.

Since it is highly challenging to characterize surface coatings inside sunscreens due to the high organic background present in the matrix, it was impossible to quantify to which extent the surface coating is altered

494 during the extraction procedure. Nonetheless, the fact that we could detect several coatings typical for TiO_2
495 particles used in sunscreens indicates that the proposed extraction method does not alter the surface coating or, at
496 least, partially preserve it. Furthermore, the characterization of the nanoparticles extracted in this study suggests
497 some similarities in terms of size, shape and surface composition between the extracted nanoparticles and
498 ingredients used in the cosmetic industry. For instance, S1-4, S7 and S11 are similar to the NM-103, reported in
499 other studies, which has an average length of 22 nm and a broadness of 34 nm and a spherical to elongated shape
500 (10,33). On the other side, S5 and S8-9 match the description of the T-lite™ SF from BASF with an elongated
501 shape and lengths between 50-200 nm and broadness of 5-10 nm (7,9). NM-103 and T-lite™ SF are coated with
502 PDMS as most of the sunscreen extracts in the present study. However, NM-103 had an isoelectric point of 8.2,
503 which is much higher than the isoelectric points measured in our study and for T-lite™ SF (7,9). Therefore, we
504 recommend using more than one single reference material for environmental studies in order to cover a broad
505 range of nanoparticle characteristics as encounter in commercial products.
506
507 *Colloidal stability of the extracted particles*
508 A white sedimentation layer was visible after several days in the sunscreen extracts. This indicates particle
509 agglomeration, since primary TiO_2 nanoparticles smaller than 50 nm are not expected to sediment under these
510 conditions (34). In order to determine if the agglomeration in the extraction medium after several days under
511 quiescent conditions is reversible, we measured the hydrodynamic diameter using DLS directly after the
512 extraction procedure and two weeks later (**figure 4**). It has to be noted that samples were diluted and sonicated
513 before each DLS measurements in order to increase the reproducibility of the size determination. As no clear
514 increase in size was observed over this period of time, we concluded that the extracted particles are stable
515 towards aggregation (irreversible agglomeration) in the Triton X-100 solution. Therefore, the observed
516 sedimentation layer corresponds to the agglomerates which could be easily disrupted during ultrasonication prior
517 to DLS measurements. This seems to be an advantage of the proposed method, for which the dispersing agent is
518 also taking the role of the stabilizer, over previously reported methods for which agglomeration of the particles
519 in the final medium could not be controlled without adding stabilizers after the extraction procedure (21,21,24).

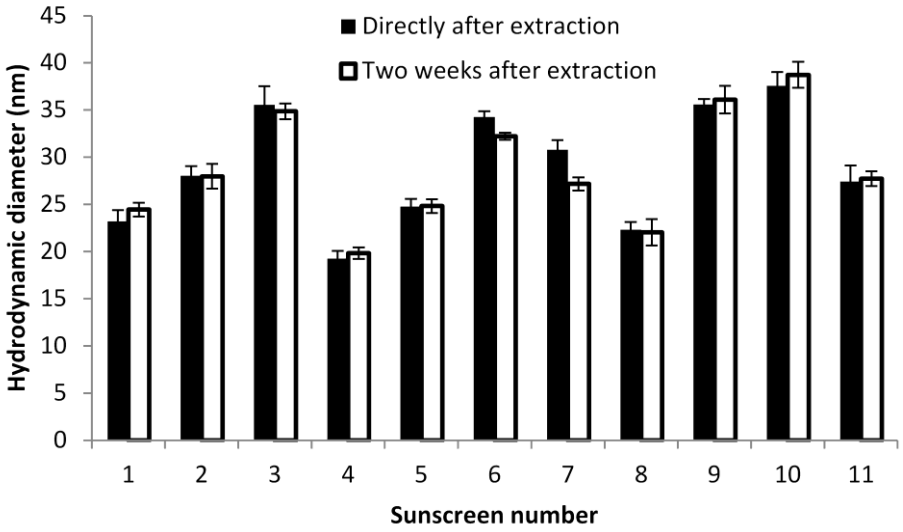

Figure 4: Hydrodynamic z-average diameter of the particles extracted from sunscreens (ultrafiltration) determined using DLS directly after the extraction (black bars) and two weeks later (white bars). The error bars denote two times the standard deviation determined from 3 replicates.

Conclusion

The tested extraction method is efficient, environmental friendly and scalable for obtaining large amount of complex TiO_2 particles at low cost. Considering the average TiO_2 content in sunscreens, it is technically possible to extract up to 10 g TiO_2 from 200 mL (one bottle) of sunscreen. These particles are extracted from commercial products and could, therefore, be used for fate and ecotoxicity studies. If the presence of surfactant in the extraction medium is expected to induce bias in such studies, the surfactant solution can be replaced by pure water by further ultrafiltration/ultracentrifugation steps. However, the suspension in the surfactant solution has the advantage to stabilize the nanoparticles which could be advantageous in some study design provided a control experiment with the corresponding surfactant solution is performed. Considering size, shape, surface charge, and coating, these particles are more environmentally relevant than pure TiO_2 nanoparticles often used as model nanoparticles. However, it remained challenging to determine if the coating is damaged during the extraction due the lack of surface characterization method for particles in their native state inside the sunscreen. Furthermore, the proposed method can also be used as a quality control method for commercial products, especially in combination with separation techniques such hydrodynamic chromatography or flow field flow fractionation for fast particle characterization. In addition, this study provides a representative overview on which types of TiO_2 nanoparticles are present in commercial sunscreens and is, therefore, informative for future risk assessment of nanoparticles in surface waters.

Acknowledgments

The authors thank the German Research Foundation (DFG) for financial support within research unit INTERNANO (FOR 1536 "Mobility, aging and functioning of engineered inorganic nanoparticles at the aquatic – terrestrial interface", subprojects SCHA849/16), the Karlsruhe Nano Micro Facility (Karlsruhe Institute of Technology) for supporting ToF-SIMS measurements, and Dr. Wolfgang Fey for the support provided during ICP-MS measurements.

References

1. Gondikas AP, Kammer F von der, Reed RB, Wagner S, Ranville JF, Hofmann T. Release of TiO2 nanoparticles from sunscreens into surface waters: a one-year survey at the old Danube recreational Lake. Environmental Science & Technology. ACS Publications; 2014;48(10):5415–22.

2. Kiser M, Westerhoff P, Benn T, Wang Y, Perez-Rivera J, Hristovski K. Titanium nanomaterial removal and release from wastewater treatment plants. Environmental Science & Technology. ACS Publications; 2009;43(17):6757–63.

3. Sharma VK. Aggregation and toxicity of titanium dioxide nanoparticles in aquatic environment—A Review. Journal of Environmental Science and Health, Part A. Taylor & Francis; 2009;44(14):1485–95.

4. Schaumann GE, Philippe A, Bundschuh M, Metreveli G, Klitzke S, Rakcheev D, et al. Understanding the fate and biological effects of Ag-and TiO 2-nanoparticles in the environment: the quest for advanced analytics and interdisciplinary concepts. Science of The Total Environment. Elsevier; 2015;535:3–19.

5. Liu HH, Cohen Y. Multimedia environmental distribution of engineered nanomaterials. Environmental Science & Technology. ACS Publications; 2014;48(6):3281–92.

6. Lewicka ZA, Benedetto AF, Benoit DN, William WY, Fortner JD, Colvin VL. The structure, composition, and dimensions of TiO2 and ZnO nanomaterials in commercial sunscreens. Journal of Nanoparticle Research. Springer; 2011;13(9):3607–17.

7. Labille J, Feng J, Botta C, Borschneck D, Sammut M, Cabie M, et al. Aging of TiO2 nanocomposites used in sunscreen. Dispersion and fate of the degradation products in aqueous environment. Environmental Pollution. Elsevier; 2010;158(12):3482–9.

8. Jaroenworaluck A, Sunsaneeyametha W, Kosachan N, Stevens R. Characteristics of silica-coated TiO2 and its UV absorption for sunscreen cosmetic applications. Surface and Interface Analysis. Wiley Online Library; 2006;38(4):473–7.

9. Auffan M, Pedeutour M, Rose J, Masion A, Ziarelli F, Borschneck D, et al. Structural degradation at the surface of a TiO2-based nanomaterial used in cosmetics. Environmental Science & Technology. ACS Publications; 2010;44(7):2689–94.

10. Nickel C, Hellack B, Nogowski A, Babick F, Stintz M, Maes H, et al. Mobility, fate and behavior of TiO2 nanomaterials in different environmental media. Environmental Research of the Federal Ministry for the Environment. 2012;

11. Gottschalk F, Lassen C, Kjoelholt J, Christensen F, Nowack B. Modeling flows and concentrations of nine engineered nanomaterials in the Danish environment. Int J Environ Res Public Health. Multidisciplinary Digital Publishing Institute; 2015;12(5):5581–602.

12. Poda A, Bednar A, Kennedy A, Harmon A, Hull M, Mitrano D, et al. Characterization of silver nanoparticles using flow-field flow fractionation interfaced to inductively coupled plasma mass spectrometry. Journal of Chromatography A. Elsevier; 2011;1218(27):4219–25.

13. Schmidt B, Loeschner K, Hadrup N, Mortensen A, Sloth JJ, Bender Koch C, et al. Quantitative characterization of gold nanoparticles by field-flow fractionation coupled online with light scattering detection and inductively coupled plasma mass spectrometry. Analytical Chemistry. ACS Publications; 2011;83(7):2461–8.

14. Gray EP, Coleman JG, Bednar AJ, Kennedy AJ, Ranville JF, Higgins CP. Extraction and analysis of silver and gold nanoparticles from biological tissues using single particle inductively coupled plasma mass spectrometry. Environmental Science & Technology. ACS Publications; 2013;47(24):14315–23.

15. Krystek P, Brandsma S, Leonards P, de Boer J. Exploring methods for compositional and particle size analysis of noble metal nanoparticles in Daphnia magna. Talanta. Elsevier; 2016;147:289–95.

16. Dan Y, Zhang W, Xue R, Ma X, Stephan C, Shi H. Characterization of gold nanoparticle uptake by tomato plants using enzymatic extraction followed by single-particle inductively coupled plasma-mass spectrometry analysis. Environmental Science & Technology. ACS Publications; 2015;49(5):3007–14.

17. Loeschner K, Navratilova J, Købler C, Mølhave K, Wagner S, von der Kammer F, et al. Detection and characterization of silver nanoparticles in chicken meat by asymmetric flow field flow fractionation with detection by conventional or single particle ICP-MS. Analytical and Bioanalytical Chemistry. Springer; 2013;405(25):8185–95.

18. Whitley AR, Levard C, Oostveen E, Bertsch PM, Matocha CJ, von der Kammer F, et al. Behavior of Ag nanoparticles in soil: effects of particle surface coating, aging and sewage sludge amendment. Environmental Pollution. Elsevier; 2013;182:141–9.

19. Contado C, Pagnoni A. TiO2 in commercial sunscreen lotion: flow field-flow fractionation and ICP-AES together for size analysis. Analytical Chemistry. ACS Publications; 2008;80(19):7594–608.

20. Cuddy MF, Poda AR, Moser RD, Weiss CA, Cairns C, Steevens JA. A weight-of-evidence approach to identify nanomaterials in consumer products: a case study of nanoparticles in commercial sunscreens. Journal of Exposure Science and Environmental Epidemiology. Nature Publishing Group; 2015;

21. Nischwitz V, Goenaga-Infante H. Improved sample preparation and quality control for the characterisation of titanium dioxide nanoparticles in sunscreens using flow field flow fractionation on-line with inductively coupled plasma mass spectrometry. Journal of Analytical Atomic Spectrometry. Royal Society of Chemistry; 2012;27(7):1084–92.

22. López-Heras I, Madrid Y, Cámara C. Prospects and difficulties in TiO 2 nanoparticles analysis in cosmetic and food products using asymmetrical flow field-flow fractionation hyphenated to inductively coupled plasma mass spectrometry. Talanta. Elsevier; 2014;124:71–8.

23. Mori Y. Size-selective separation techniques for nanoparticles in liquid. KONA Powder and Particle Journal. Hosokawa Powder Technology Foundation; 2015;32(0):102–14.

24. Bairi VG, Lim J-H, Fong A, Linder SW. Size characterization of metal oxide nanoparticles in commercial sunscreen products. Journal of Nanoparticle Research. Springer; 2017;19(7):256.

25. Lee JN, Park C, Whitesides GM. Solvent compatibility of poly(dimethylsiloxane)-based microfluidic devices. Analytical chemistry. 2003;75(23):6544–54.

26. Chen X, Mao SS. Titanium dioxide nanomaterials: synthesis, properties, modifications, and applications. Chemical Reviews. ACS Publications; 2007;107(7):2891–959.

27. Klang V, Matsko NB, Valenta C, Hofer F. Electron microscopy of nanoemulsions: an essential tool for characterisation and stability assessment. Micron. 2012;43(2-3):85–103.

28. Kosmulski M. Isoelectric points and points of zero charge of metal (hydr) oxides: 50years after Parks' review. Adv Colloid Interface Sci. Elsevier; 2016;

29. Hunter RJ. Foundations of Colloid Science . Second Edition. Oxford University, editor. Oxford University Press; 2001.

30. Dong X, Gusev A, Hercules DM. Characterization of polysiloxanes with different functional groups by time-of-flight secondary ion mass spectrometry. Journal of the American Society for Mass Spectrometry. Elsevier; 1998;9(4):292–8.

31. Szakal C, McCarthy JA, Ugelow MS, Konicek AR, Louis K, Yezer B, et al. Preparation and measurement methods for studying nanoparticle aggregate surface chemistry. Journal of Environmental Monitoring. Royal Society of Chemistry; 2012;14(7):1914–25.

32. Niibori Y, Kunita M, Tochiyama O, Chida T. Dissolution rates of amorphous silica in highly alkaline solution. Journal of Nuclear Science and Technology. Taylor & Francis; 2000;37(4):349–57.

33. Rasmussen K, Mast J, De Temmerman P-J, Verleysen E, Waegeneers N, Van Steen F, et al. Titanium dioxide, NM-100, NM-101, NM-102, NM-103, NM-104, NM-105: characterisation and physico-chemical properties. JRC Science and Policy Reports. 2014;

34. Alexander CM, Dabrowiak JC, Goodisman J. Gravitational sedimentation of gold nanoparticles. J Colloid Interface Sci. 2013;396:53–62.